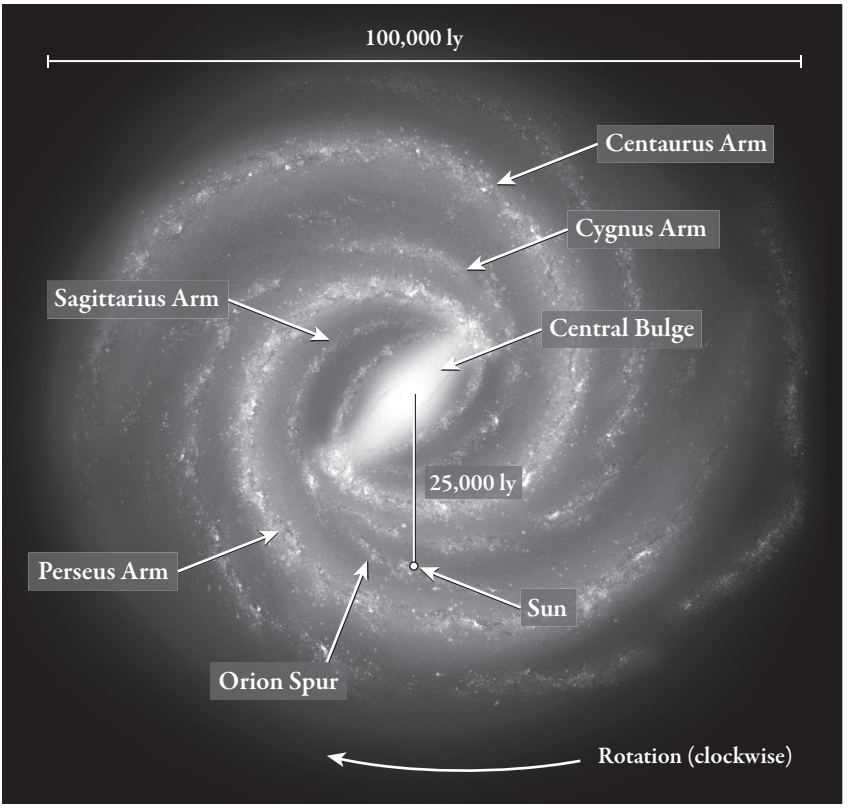

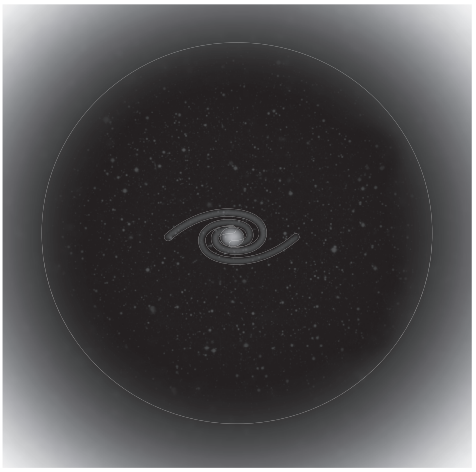

FIGURE 2.2 The Milky Way. (Top) The pinwheel shape of the spiral arms of the disk of the Galaxy is shown in the drawing. The central bright region is the Galactic Bulge, a central region of tightly packed stars. At the very center of the Galaxy is Sagittarius A*, a strong radio source affiliated with a black hole weighing 4 million times as much as our Sun. The Sun is located about 25,000 light-years away from the Galactic Center. (Bottom) Artist's rendition of a galaxy, showing the spiral structure of the disk as well as the much larger spherical dark matter halo. *(Top) NASA/JPL-CalTech.*

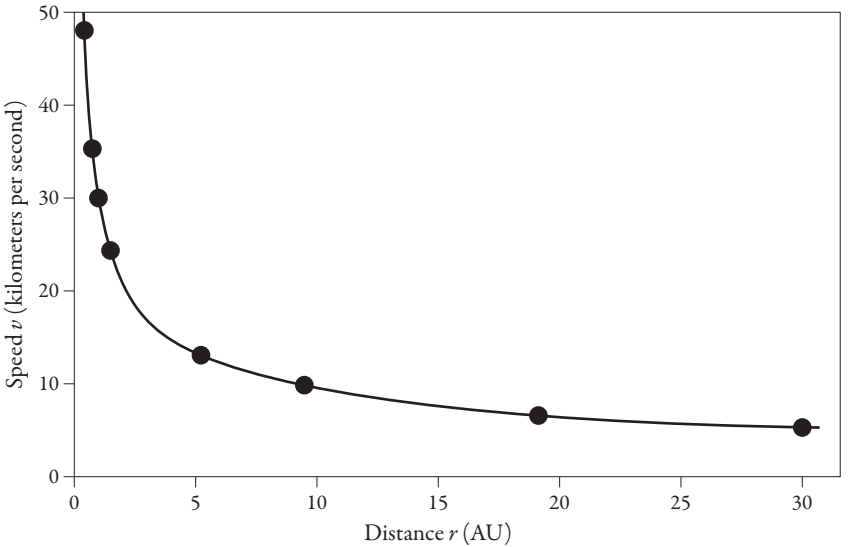

FIGURE 2.3 The rotation curve of the Solar System: average speeds of the planets versus distance from the Sun. The Sun (not shown in the plot) is located at $r = 0$; the planets are at distances as indicated in astronomical units (AU). One AU is the distance between Earth and the Sun, roughly 100 million kilometers. The farther out a planet is from the Sun, the more slowly it revolves in its orbit.

FIGURE 2.4 Tycho Brahe (1546–1601). He lost his nose in a duel and wore a gold-and-silver replacement. Brahe is known for his studies of planetary orbits.

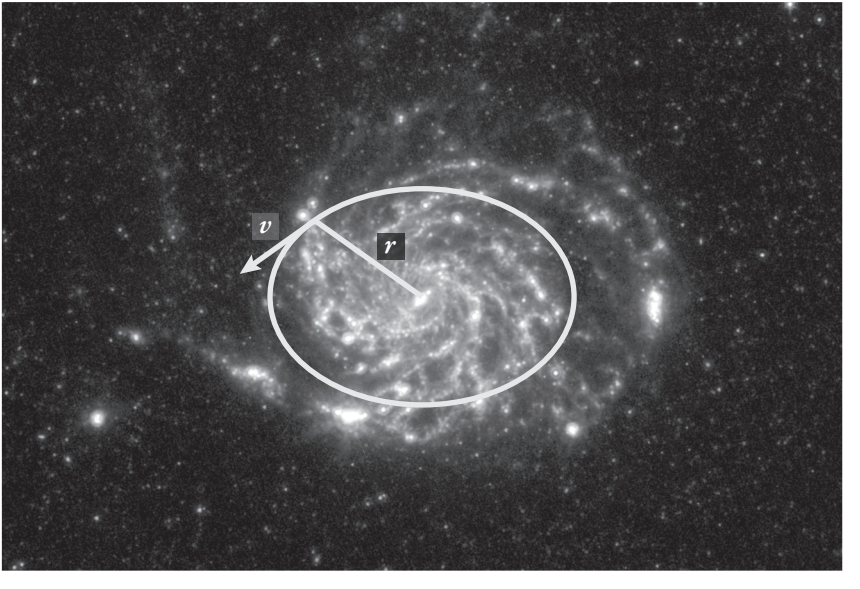

FIGURE 2.5 The path of a star in a circular orbit around the center of a galaxy. The orbital speed v is determined by the amount of mass interior to the orbit at radius r. *NASA/JPL-Caltech/STScI.*

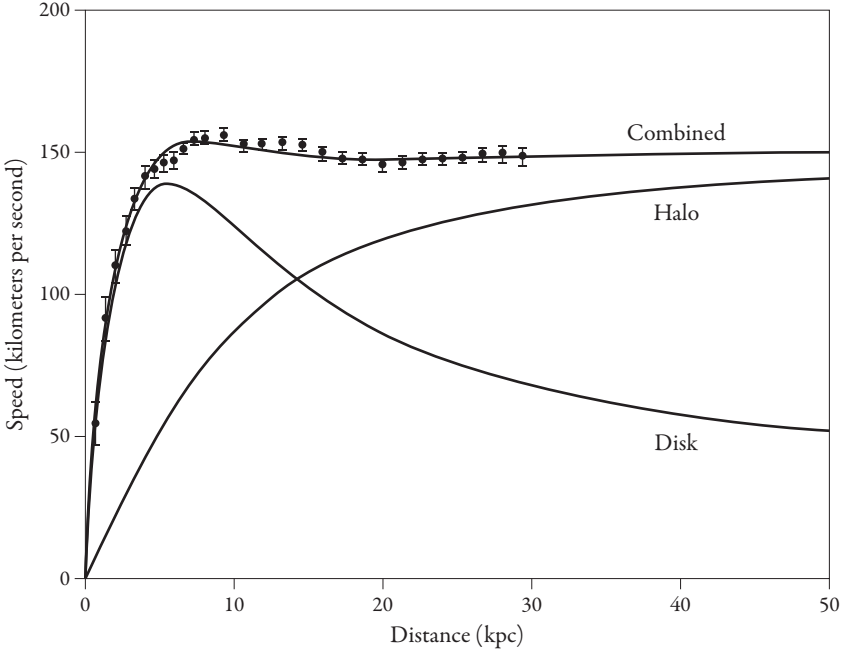

FIGURE 2.6 The rotation curve of galaxy NGC 3198. Radial distances are measured in units of kiloparsecs (kpc), or thousands of parsecs; a parsec corresponds to roughly 30 trillion kilometers (19 trillion miles). The dots with bars show the observational data, whereas the solid curves show the calculated contributions from the stellar disk, the dark matter halo, and the two combined. Dark matter is required to explain the data. *Redrawn from van Albada, T. S., J. N. Bahcall, K. Begeman, and R. Sancisi. 1985. "Distribution of Dark Matter in the Spiral Galaxy NGC 3198."* Astrophysical Journal *295: 305.*

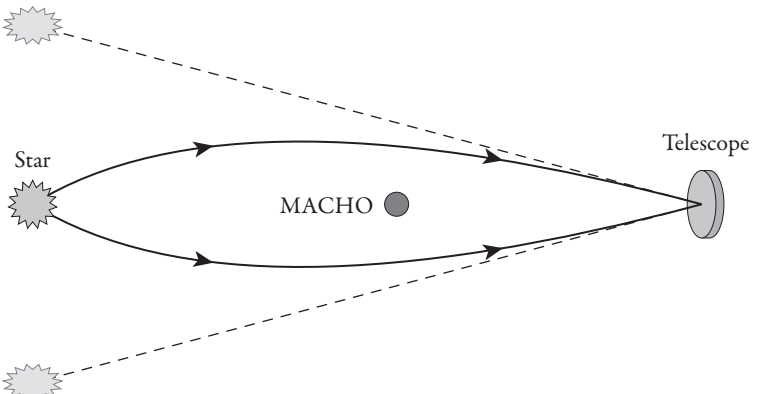

FIGURE 2.8 Gravitational lensing: a Massive Compact Halo Object (MACHO) bends the light of a distant star seen by a telescope on Earth. Whereas the actual star is located directly behind the MACHO, the telescopes see what appear to be two distorted images at different locations than the real star. Any intervening mass between the star and the telescope would have the same lensing effect.

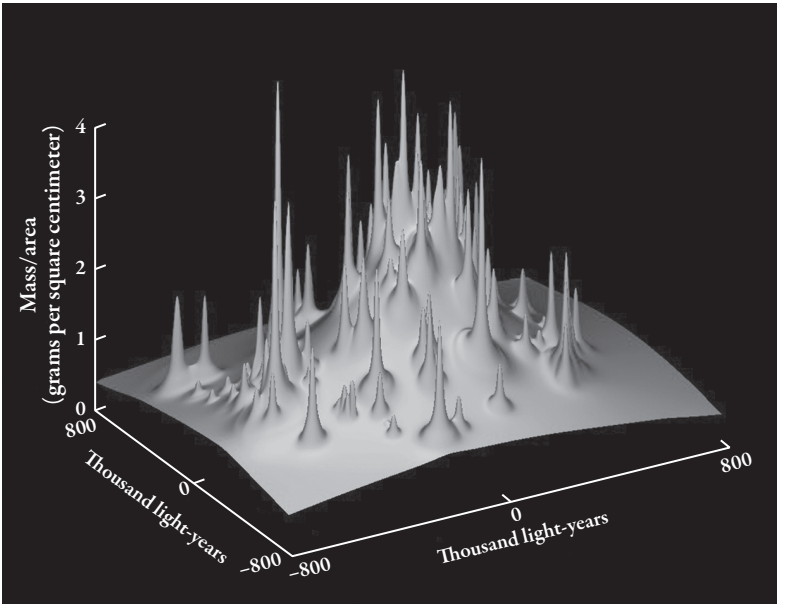

FIGURE 2.11 (A color version of this figure is included in the insert following page 82.) Computer reconstructed image of the mass distribution in galaxy cluster CL0024+1654, based on data from the Hubble Space Telescope. This massive cluster gravitationally lensed the light of a more distant bright galaxy, producing multiple images of the source galaxy and allowing scientists to reconstruct the hidden mass inside the cluster. The peaks in the image are galaxies; the bulk of the mass consists of the central mountain made of dark matter in between the galaxies. *From Tyson, J. A., G. P. Kochanski, and I. P. Dell'Antonio. 1998.* Astrophysical Journal Letters *498: L107.*

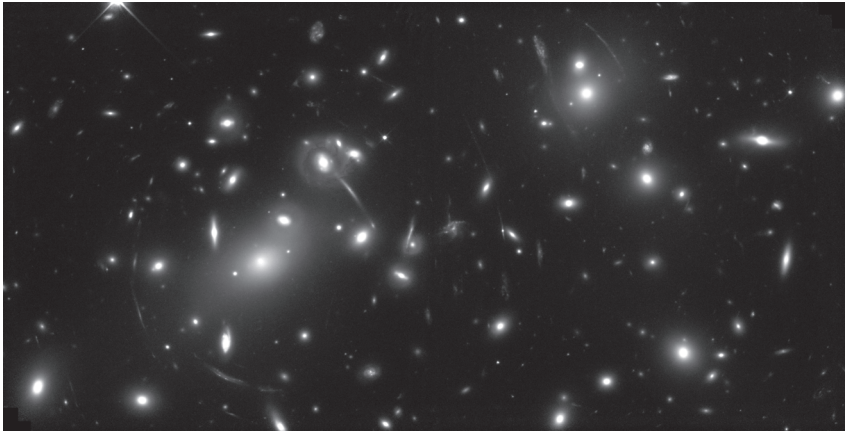

FIGURE 2.12 Galaxy cluster Abell 2218 acts as a powerful lens. It is so massive that its gravity bends, magnifies, and distorts the light from galaxies lying behind the cluster into elongated arcs and multiple images. This image is from data taken with the Hubble Space Telescope. *NASA, Andrew Fruchter and the ERO Team [Sylvia Baggett (STScI), Richard Hook (ST-ECF), Zoltan Levay (STScI)] (STScI).*

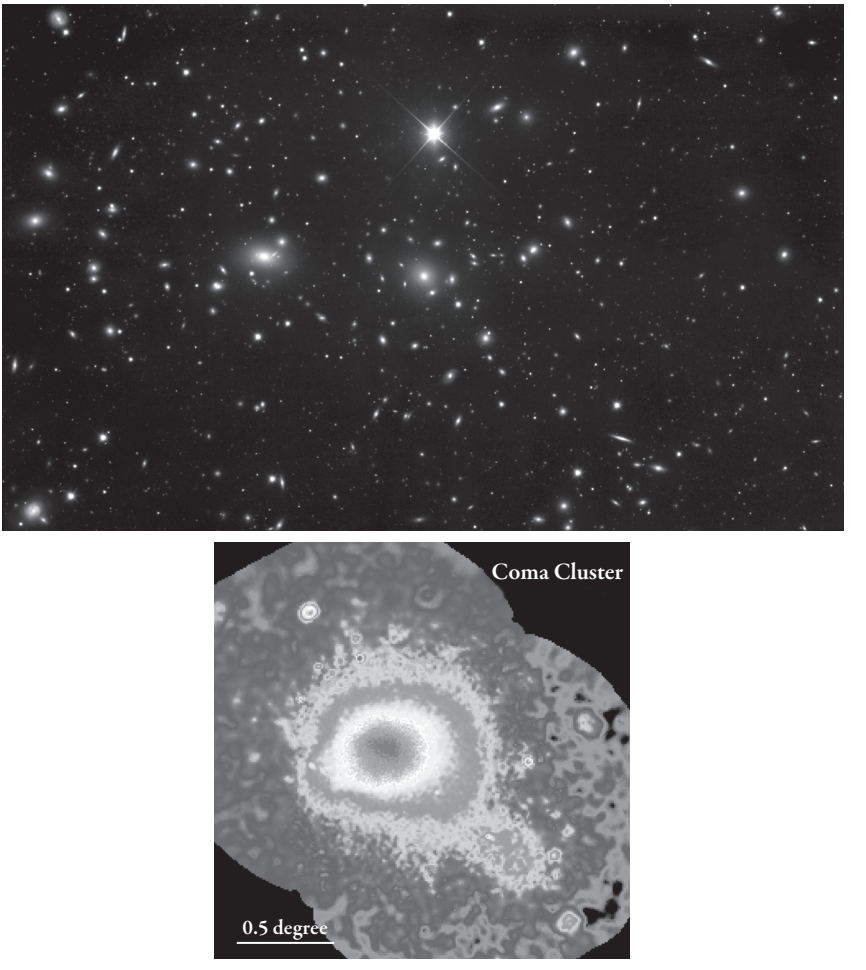

FIGURE 2.13 (A color version of this figure is included in the insert following page 82.) Galaxy cluster Coma provides evidence for dark matter. The x-rays in the image on the bottom are produced by hot gas, which would have evaporated from the cluster without the gravity provided by an enormous dark matter component in the cluster. (Top) Optical image. (Bottom) X-ray image. The two images are not on the same scale; the x-ray image focuses on the central region of the cluster. *(Top) NASA, ESA, and the Hubble Heritage Team (STScI/AURA); (bottom) ROSAT/MPE/S. L. Snowden.*

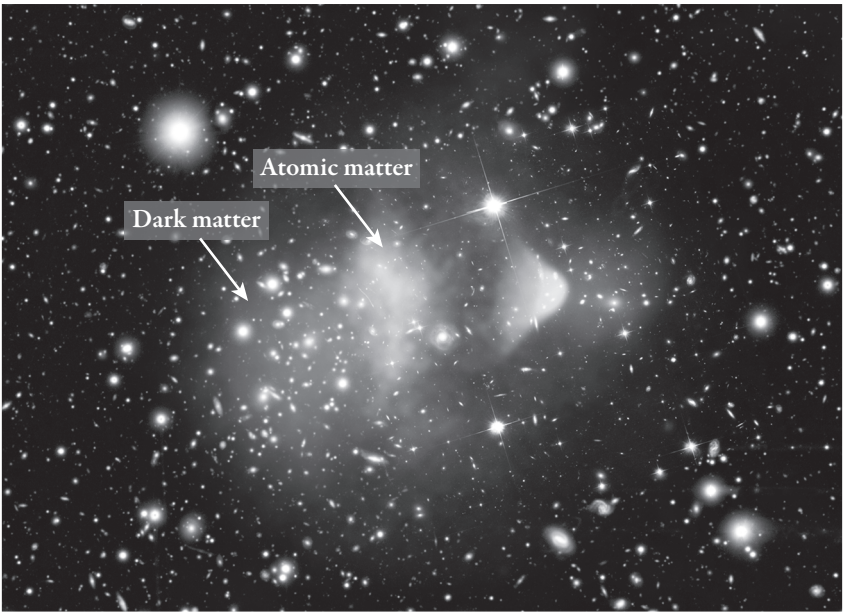

FIGURE 2.14 (A color version of this figure is included in the insert following page 82.) The Bullet Cluster, a merger of two clusters each containing dozens of galaxies, gives striking confirmation of the existence of dark matter. In the color version of the figure, the dark matter from lensing measurements is shown in blue; the x-ray gas composed of atomic matter is shown in red. The separation of the two components occurs because the atomic gas decelerates when it collides at the center, but the collisionless dark matter passes right on through. The existence of these two independent components is exactly as predicted in dark matter theories. The name "Bullet Cluster" refers to the striking illusion that one of the clusters looks like a bullet piercing the other. *(X-ray) NASA/CXC/CfA/M. Markevitch et al.; (lensing map) NASA/STScI, ESO WFI, Magellan/U. Arizona/D. Clowe et al.; (optical) NASA/STScI, Magellan/U. Arizona/D. Clowe et al.*

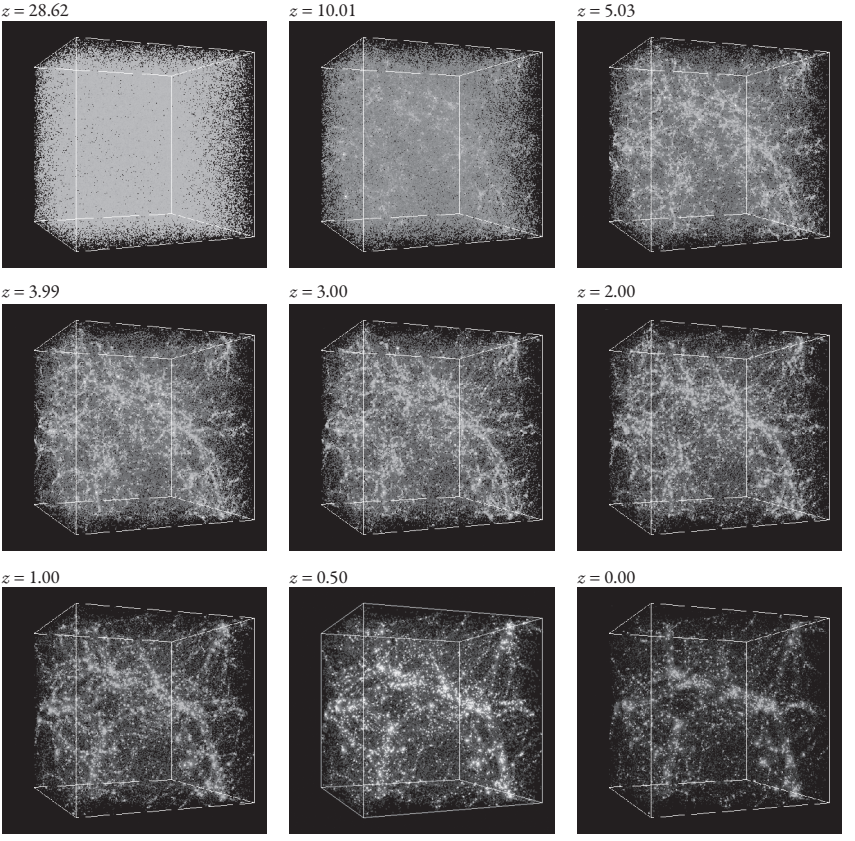

FIGURE 2.15 (A color version of this figure is included in the insert following page 82.) Computer simulation of galaxy formation starting from 100 million years after the Big Bang ($z = 28.62$). The time sequence is labeled in terms of the redshift z, where higher values of z correspond to earlier times in the Universe ($z = 0$ today). The bright regions in the images are actually the locations of dark matter; as the dominant matter in the Universe, it controls the formation of large-scale structure. The first small clumps of dark matter merged to form ever-larger objects, eventually creating the galaxies and other large structures we see today. Galaxies are located at the intersections of the long stringy filaments shown in the final images. Without dark matter, galaxies would never have formed and we would not exist! *Simulations were performed at the National Center for Supercomputer Applications by Andrey Kravtsov (University of Chicago) and Anatoly Klypin (New Mexico State University). Visualizations by Andrey Kravtsov.*

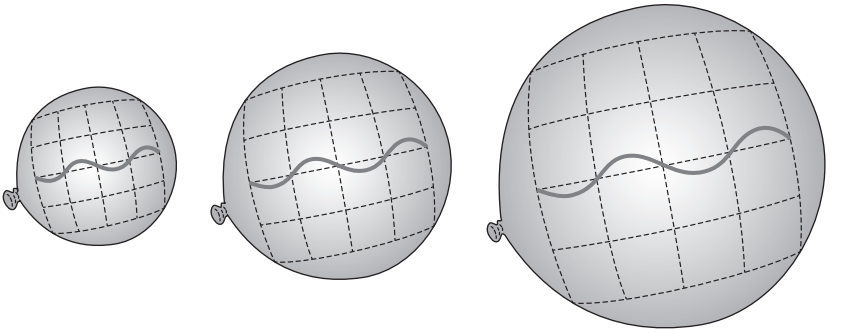

FIGURE 3.1 Wavelengths of light stretch as the Universe expands, as shown by analogy with an expanding balloon.

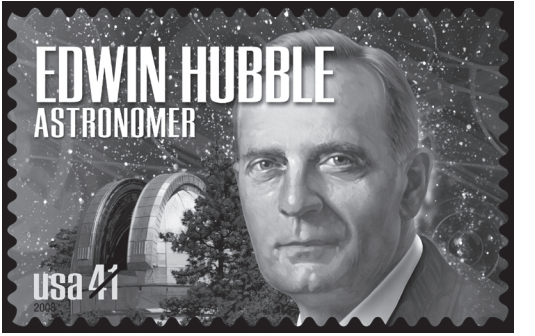

FIGURE 3.2 In 2008 the U.S. Postal Service released a 41-cent stamp honoring Hubble with the following citation: "Often called a 'pioneer of the distant stars,' astronomer Edwin Hubble (1889–1953) played a pivotal role in deciphering the vast and complex nature of the universe. His meticulous studies of spiral nebulae proved the existence of galaxies other than our own Milky Way. Had he not died suddenly in 1953, Hubble would have won that year's Nobel Prize in Physics." *USPS/Victor Stabin.*

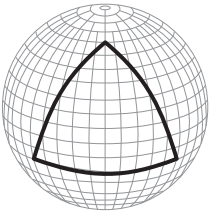

Spherical geometry

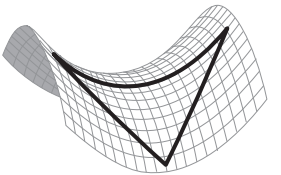

Hyperboloid (saddle) geometry

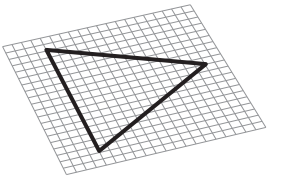

Flat geometry

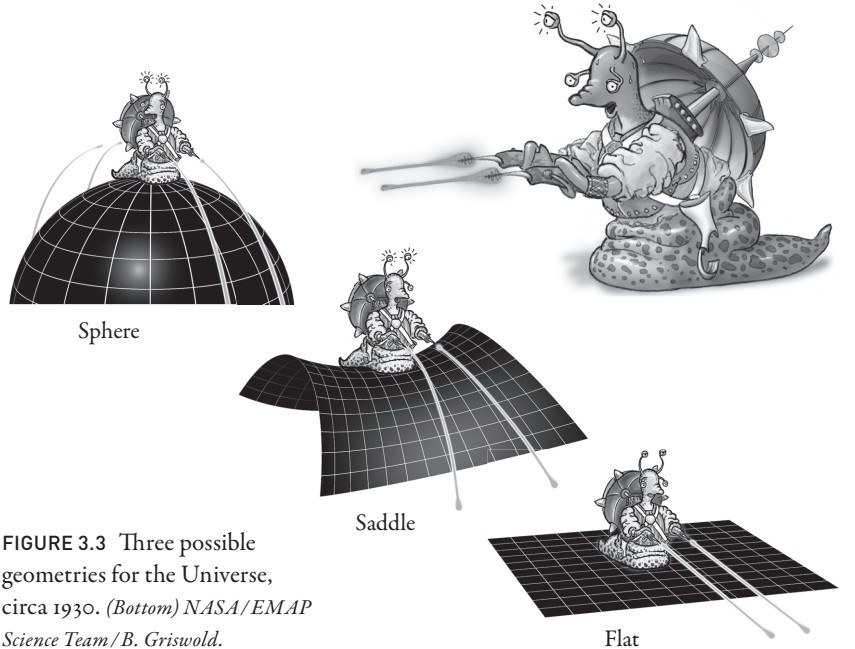

FIGURE 3.3 Three possible geometries for the Universe, circa 1930. *(Bottom) NASA/EMAP Science Team/B. Griswold.*

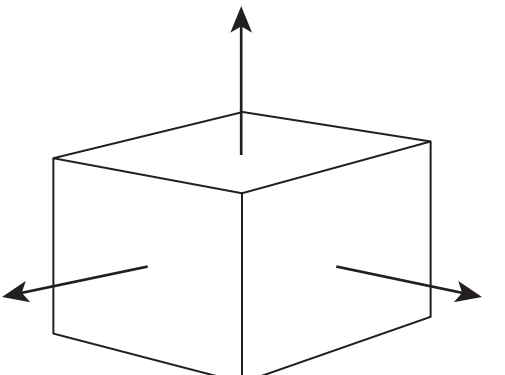

FIGURE 3.4 A Universe with a flat geometry is not two dimensional. Instead, it goes out to infinity in all three directions (as indicated by the arrows). "Flat" refers to the fact that the Universe has no curvature.

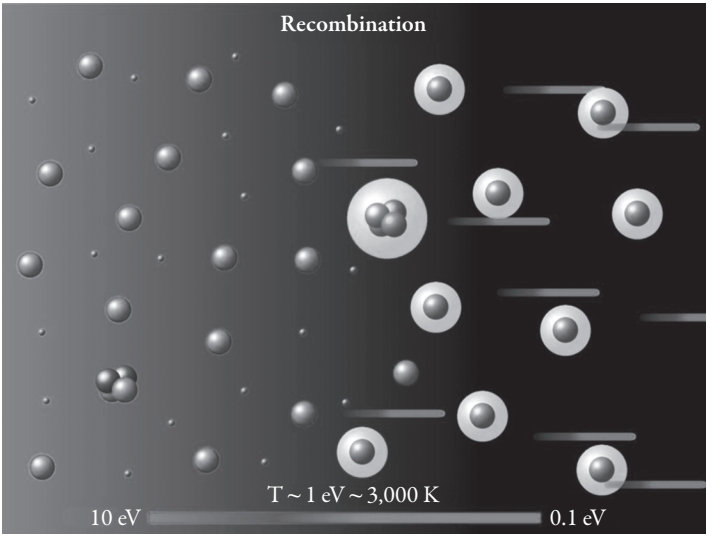

FIGURE 3.5 Origin of the cosmic microwave background (time moves from left to right). Photons (light particles) scattered off of electrons until recombination at a temperature of 3,000 K; after that the free electrons combined with protons to form neutral hydrogen atoms. From that time the photons (indicated as streaks) travel to us unimpeded and today are detected as microwaves. *Professor William Kinney of the University at Buffalo.*

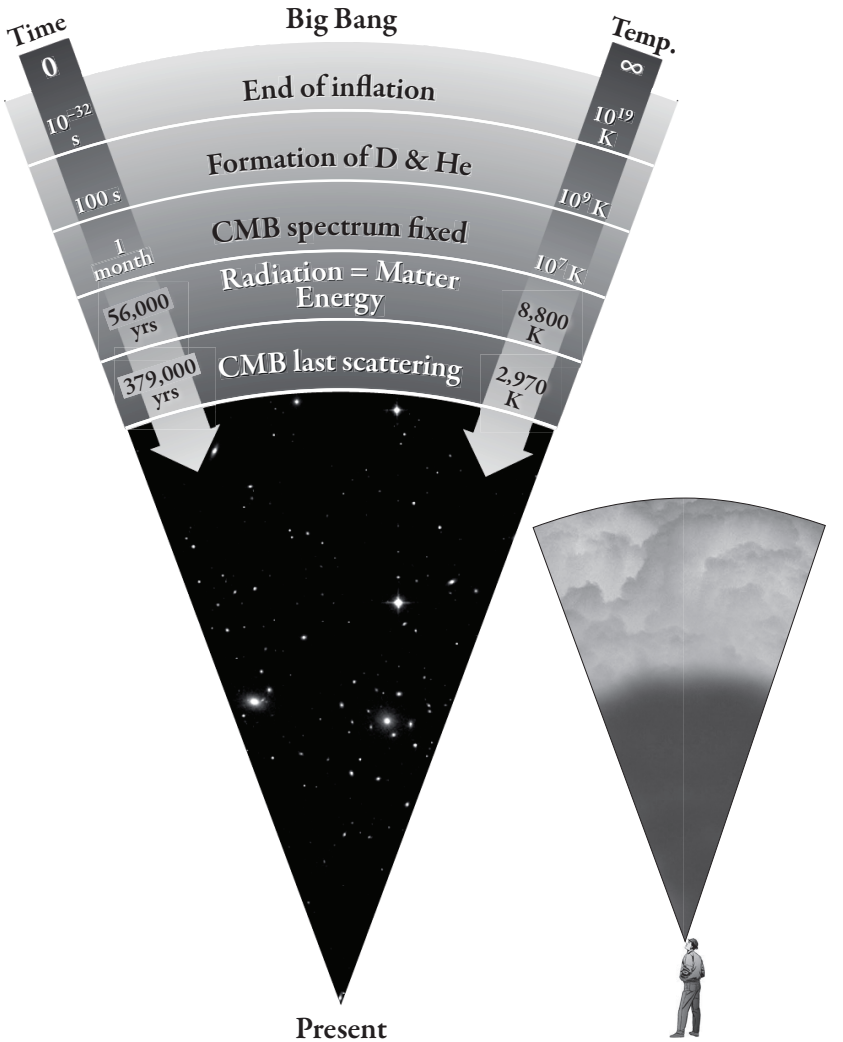

FIGURE 3.6 Photons travel to us unimpeded from the surface of last scattering, when they last interacted with electrons. This surface is analogous to a layer of clouds. In both cases, we can see only as far out as the surface corresponding to the last time light scattered. *NASA.*

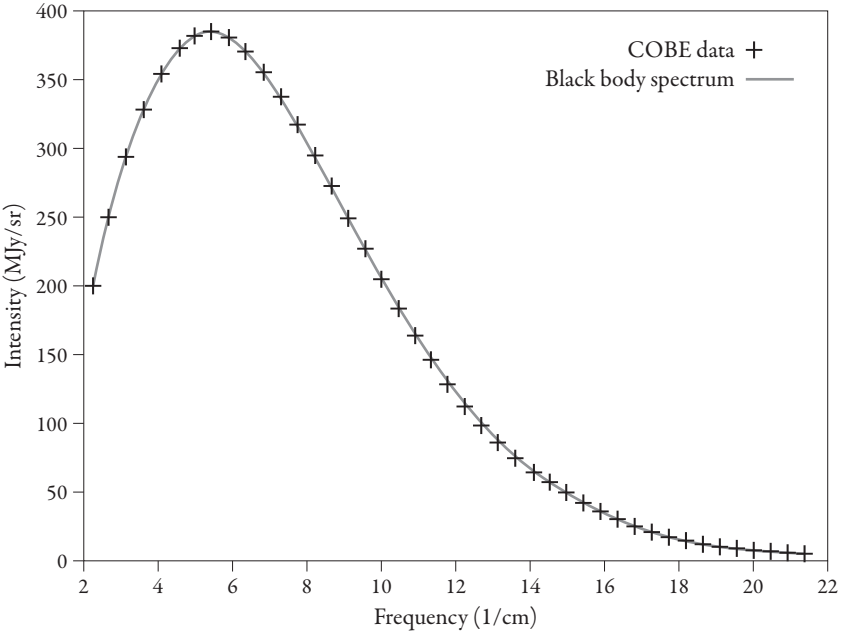

FIGURE 3.7 Blackbody spectrum of the cosmic microwave background. The plot shows the intensity of light versus the frequency (higher frequency corresponds to shorter wavelength). Theoretical predictions (solid line) perfectly match data (crosses) taken in 1990 by the Cosmic Background Explorer satellite. *NASA/COBE team.*

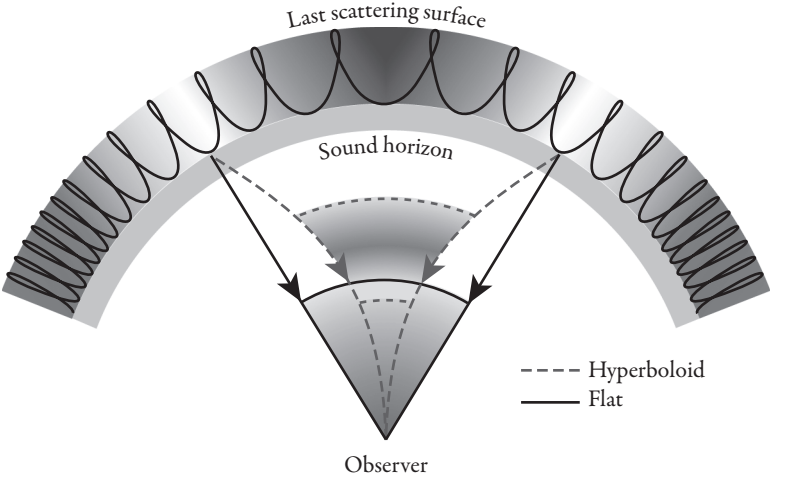

FIGURE 3.9 The sound horizon at the surface of last scattering serves as a meter stick. In a flat geometry, light rays travel in straight (solid) lines. In a hyperboloid (open) geometry, light travels along curved (dotted) lines. Measuring the angle between these lines determines the geometry of the Universe. *From Hu, W., N. Sugiyama, and J. Silk. 1997. "The Physics of Microwave Background Anisotropies."* Nature *386: 37.*

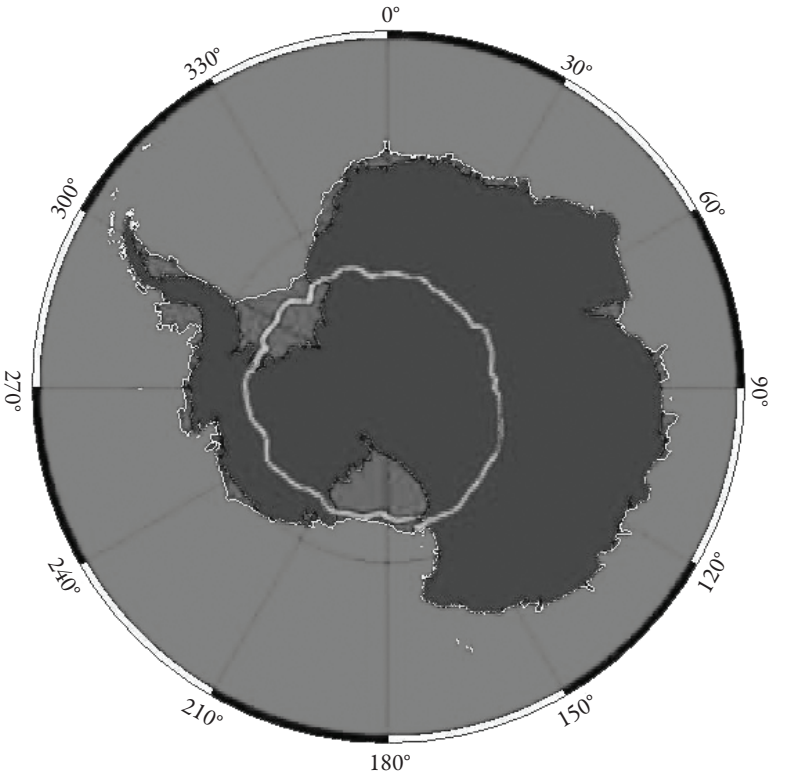

FIGURE 3.10 (A color version of this figure is included in the insert following page 82.) The path of the BOOMERANG satellite as it circumnavigated the South Pole. *The Boomerang Collaboration.*

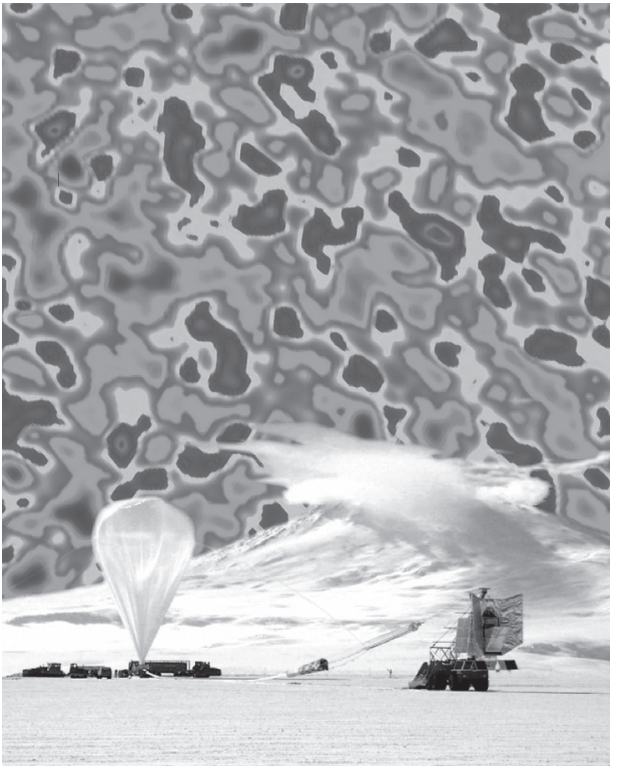

FIGURE 3.11 (A color version of this figure is included in the insert following page 82.) The BOOMERANG experiment about to be launched at the South Pole. In the background is a computer reconstruction of the microwave images it saw. From the sizes of the dark blue hot spots, scientists deciphered the shape and curvature of the Universe. *The Boomerang Collaboration.*

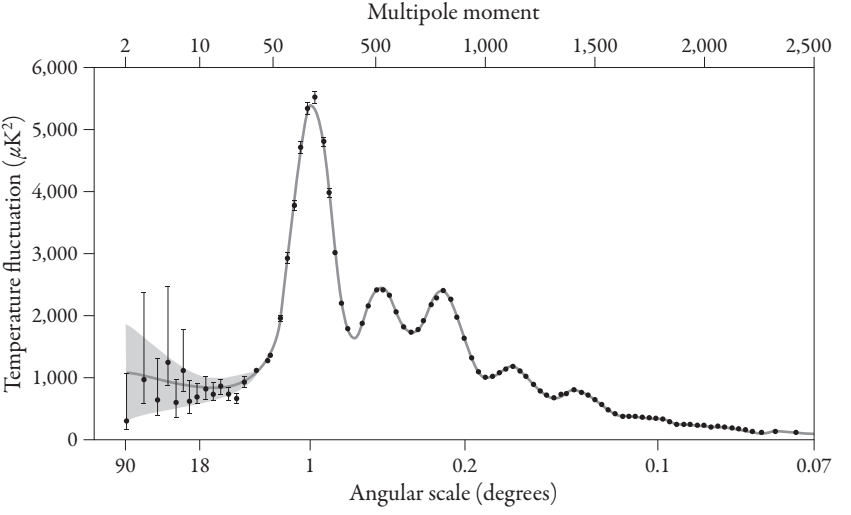

FIGURE 3.12 The Doppler peak in the cosmic microwave background (CMB) is at an angular scale of 1 degree, exactly as predicted for a Universe with a flat geometry. A combination of information from the secondary peaks (to the right of the main one) reveals the amount of atomic matter to constitute 5% of the Universe, dark matter to make up 26% of the total, and dark energy to constitute the remaining 69%. This plot is the result of data from the European Space Agency's Planck satellite from March 2013. *Reproduced with permission from* Astronomy & Astrophysics, © *ESO, original source ESA and the Planck Collaboration, P.A.R. Ade et al. [Planck Collaboration]. "Planck 2013 Results. I. Overview of Products and Scientific Results." arXiv:1303.5062 [astro-ph.CO].*

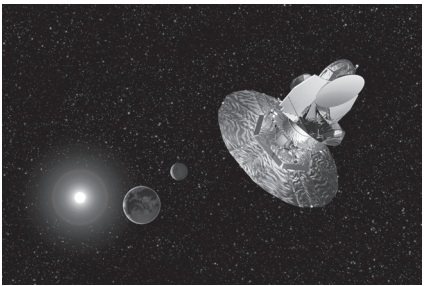

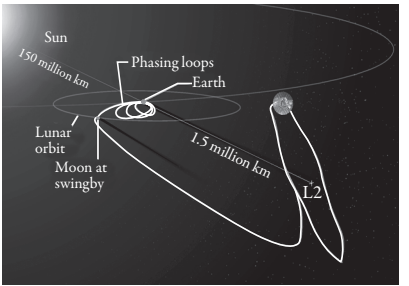

FIGURE 3.13 (Left) Data from NASA's Wilkinson Microwave Anisotropy Probe (WMAP) satellite has led to the precision era in cosmology. Yet the dark side of the Universe remains an enigma. (Right) The path taken by WMAP to get to its current location at L2, the second Lagrange point of the Sun-Earth system, where WMAP resides on a stable orbit 1 million miles from Earth. The European Space Agency's Planck satellite also resides at L2, as will the upcoming James Webb Space Telescope, the sequel to the Hubble Space Telescope. *NASA/WMAP Science Team.*

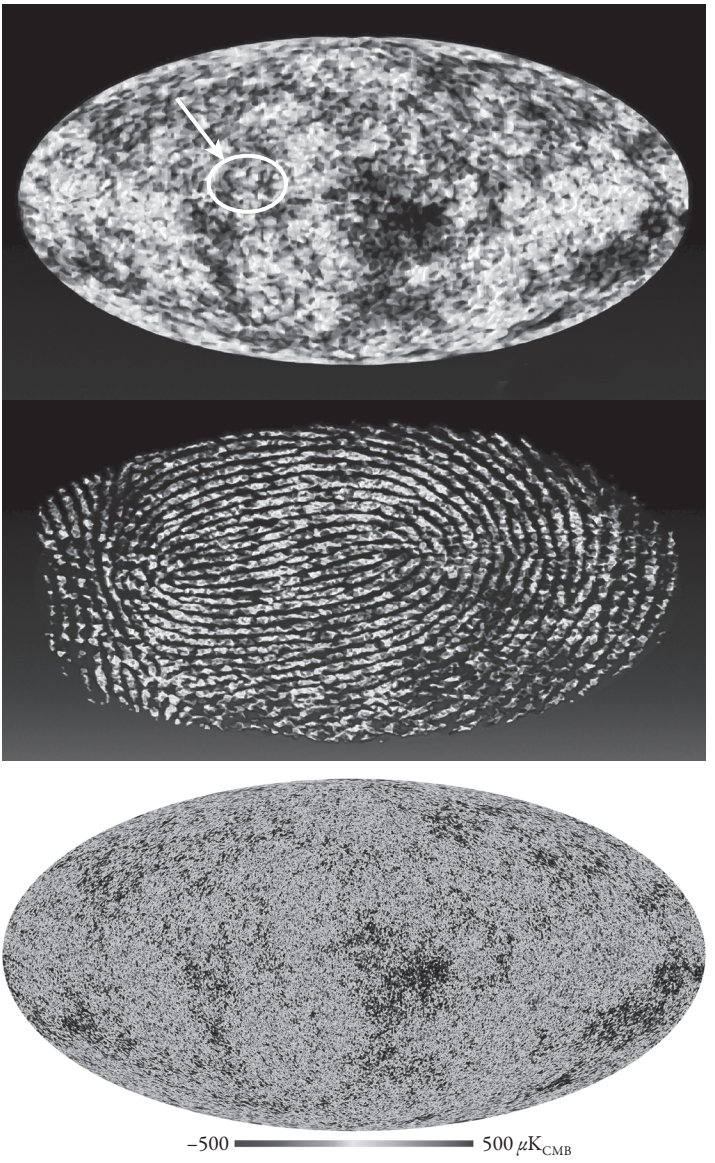

FIGURE 3.14 (A color version of this figure is included in the insert following page 82.) The microwave sky as seen by the Wilkinson Microwave Anisotropy Probe (WMAP) (top) and Planck (bottom) satellites. Hot spots are red/orange, whereas blue regions are cold (compared to the average 2.76 K temperature). The putative initials of Stephen Hawking are circled. The WMAP and Planck images are like a fingerprint of our Universe. *(Top) NASA/WMAP Science Team; (bottom) ESA/Planck Collaboration.*

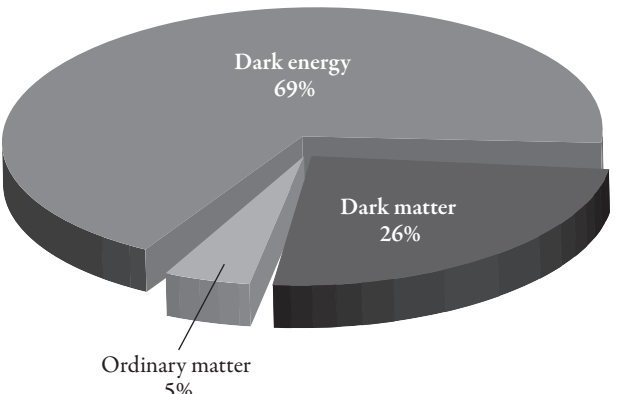

FIGURE 3.18 (A color version of this figure is included in the insert following page 82.) Pie chart of the Universe showing its three primary components.

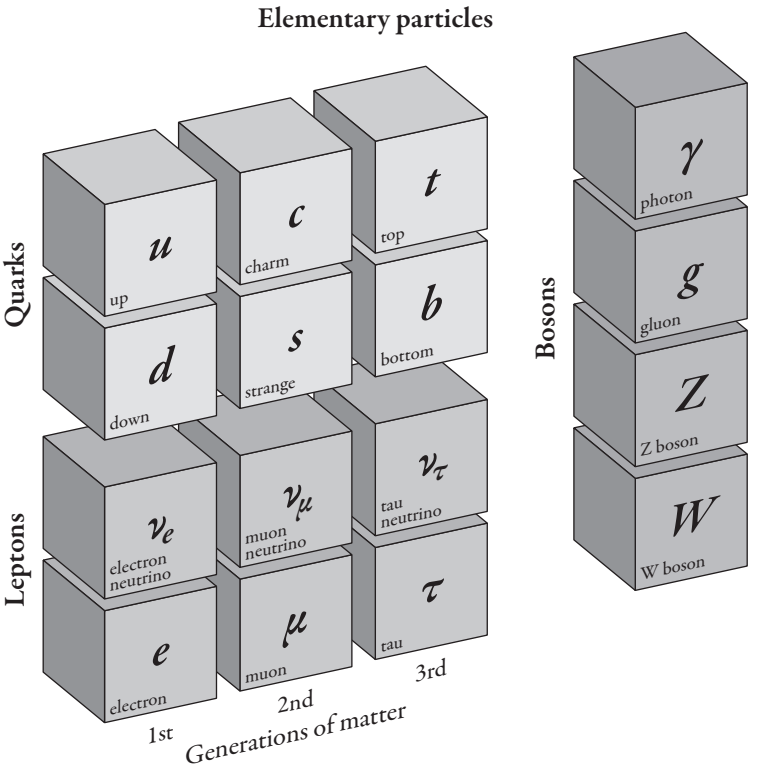

FIGURE 4.1 Three types of elementary particles are the basic building blocks of nature: quarks, leptons, and bosons. Quarks come in six types—up, down, charm, strange, top, and bottom—and combine to make objects like protons and neutrons. Gauge bosons are the particles responsible for the fundamental forces: photons mediate the electromagnetic forces that attract electrons to the protons in atomic nuclei, gluons mediate the strong force that binds together the quarks inside protons and neutrons; and Ws and Zs mediate the weak interactions that are responsible for some types of radioactivity. These elementary particles, together with the Higgs boson, constitute the Standard Model of particle physics. *Fermilab.*

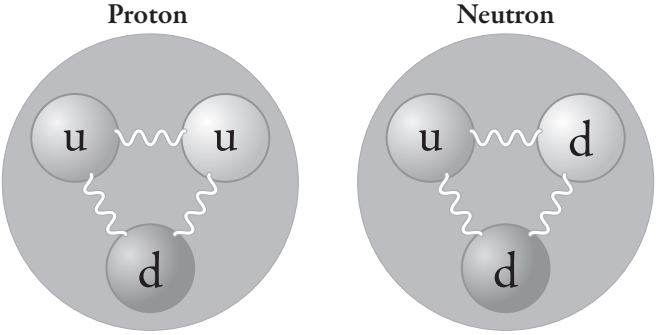

FIGURE 4.2 The quark structure of the proton and neutron. Gluons (squiggly lines) hold the quarks together.

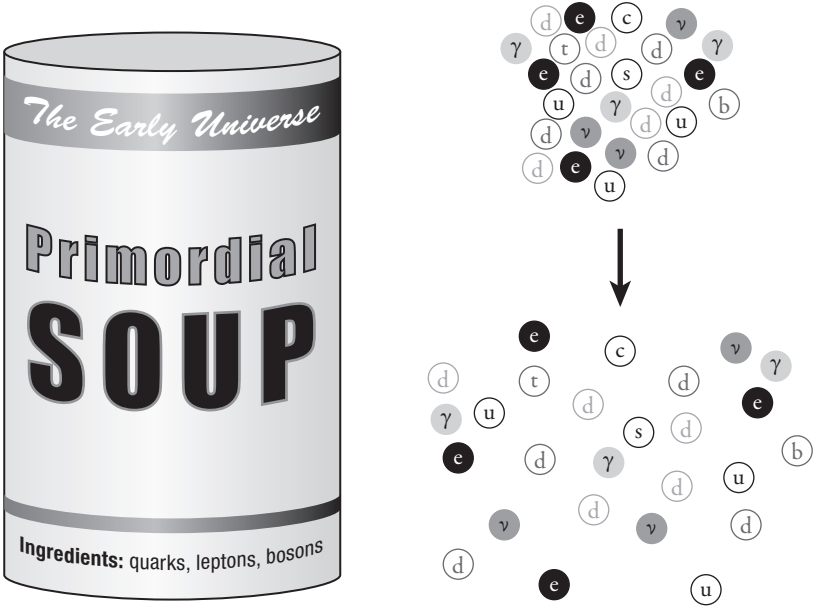

FIGURE 4.3 The early Universe was a primordial soup of quarks, leptons (such as electrons and neutrinos, symbolized by ν), and bosons (such as photons, symbolized by γ). As the Universe expanded, these particles moved farther apart and their collisions with one another became less frequent.

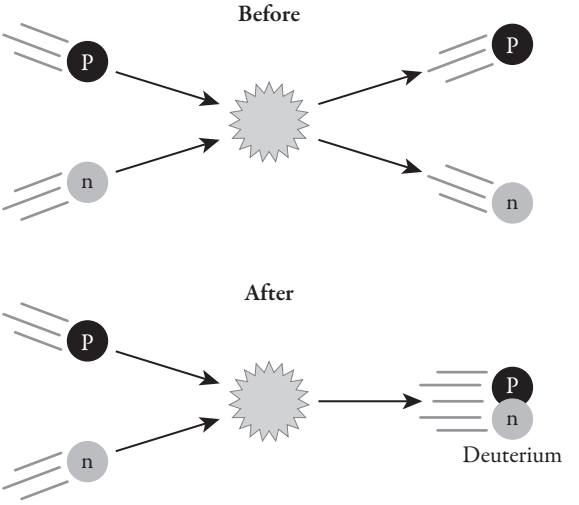

FIGURE 4.4 Before and after the first 3 minutes. The formation of elements more complex than hydrogen began with the formation of deuterium approximately 3 minutes after the Big Bang. Deuterium, which consists of one neutron and one proton, was the first building block of the other light elements. Before the Universe was 3 minutes old, deuterium wasn't stable; when it formed, it immediately dissociated again into its constituent protons and neutrons. After the Universe was 3 minutes old, deuterium became stable, triggering the beginning of Big Bang nucleosynthesis.

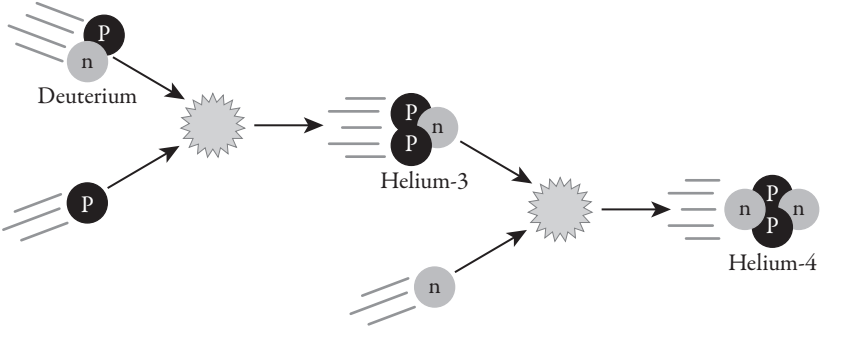

FIGURE 4.5 A pathway for the formation of helium-4 from deuterium.

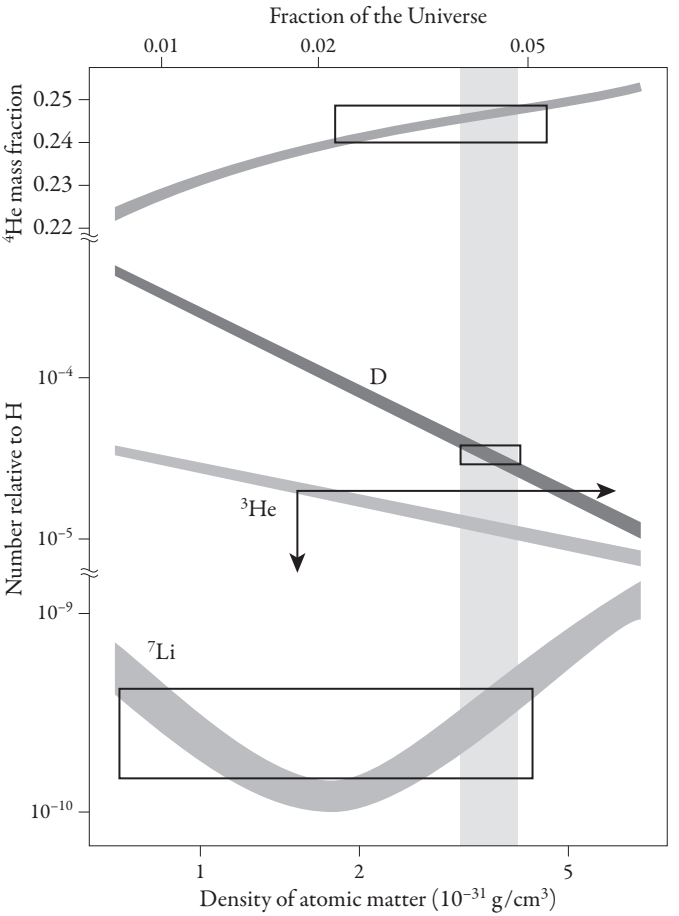

FIGURE 4.6 Abundances for the light nuclei helium-4, deuterium (D), helium-3, and lithium-7 from Big Bang nucleosynthesis. The solid curves are theoretical predictions, whereas the boxes indicate observed measurements and the arrows indicate bounds from data. Agreement requires the atomic fraction of the Universe to be only 5% of the content of the Universe. The lower horizontal axis indicates the density of atomic matter, also known as baryonic matter. *Adapted from Burles, S., K. M. Nollett, and M. S. Turner. 1999. "Big Bang Nucleosynthesis: Linking Inner Space and Outer Space." In* Heavy Ion Physics from Bevalac to RHIC. Proceedings, Relativistic Heavy Ion Symposium, APS Centennial Meeting, *edited by R. Seto. Singapore: World Scientific, 1999.*

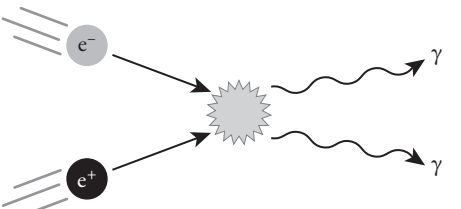

FIGURE 5.1 Annihilation of positron-electron (e^+-e^-) pair into photons (γ).

FIGURE 5.2 MACHOs are dead. Desperately seeking WIMPs. *Simon Strandgaard*.

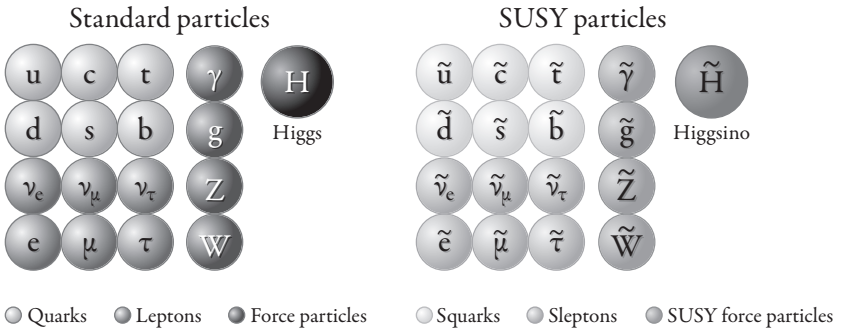

FIGURE 5.4 The supersymmetric (SUSY) extension of the Standard Model doubles the numbers of particles in the Universe. Every particle has a SUSY partner, such as the squark ($\tilde{q}$) for the quark, the photino ($\tilde{\gamma}$) for the photon, and the Higgsino for the Higgs. The tilde over the top of the letter indicates the SUSY partner. The lightest SUSY particle, probably a combination of Higgsino and SUSY force particles, is the dark matter candidate.

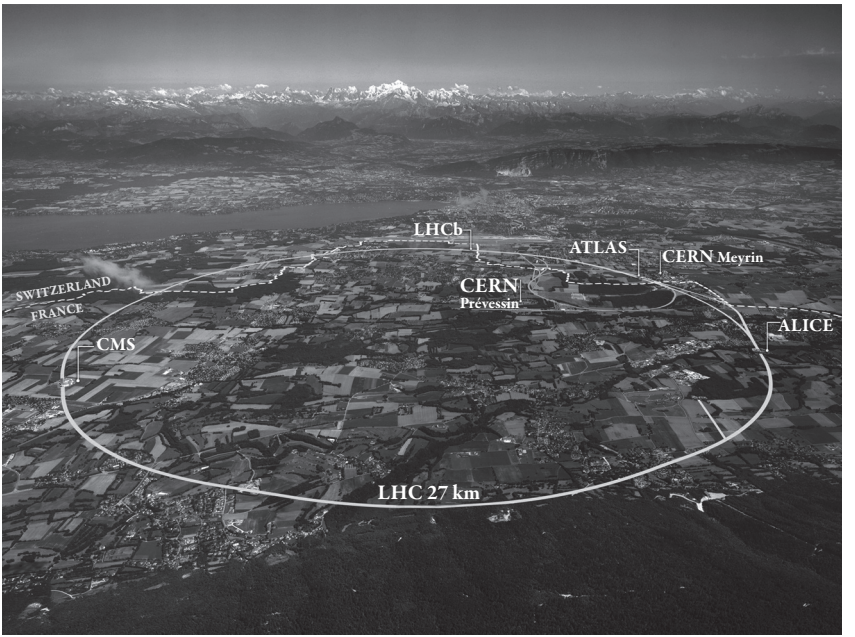

FIGURE 6.1 The Large Hadron Collider at CERN near Geneva, Switzerland. Protons are accelerated in opposite directions around the ring (drawn in on the surface of Earth) in an underground tunnel 27 kilometers (17 miles) around. CERN scientists work at two main sites: CERN Meyrin and CERN Prévessin. The particles collide at the four intersection points where the CMS, ATLAS, LHCb, and ALICE detectors are located. *CERN.*

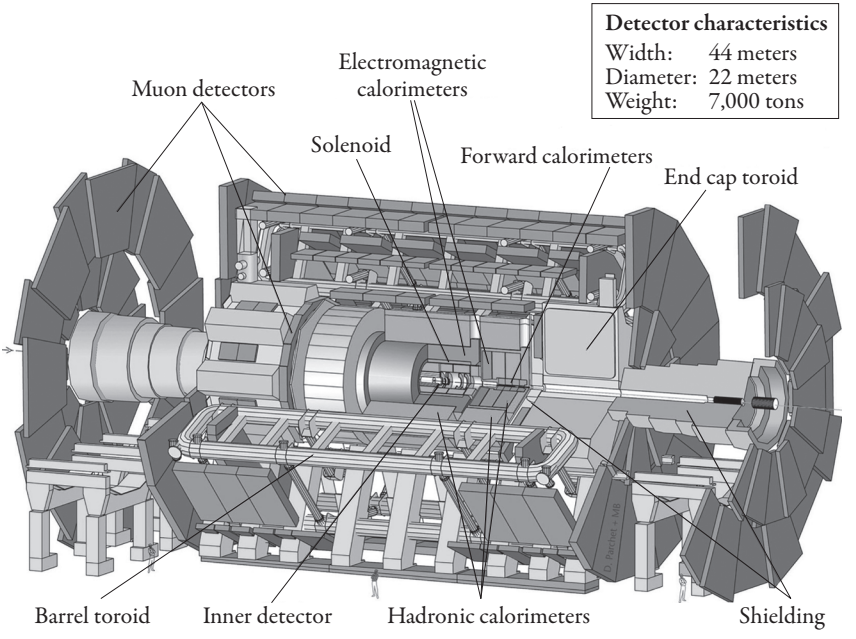

FIGURE 6.3 The ATLAS detector at CERN. The two proton beams come in from the left and right sides through the beam pipe and collide in the heart of the detector. The outgoing particles from the interaction point traverse a series of concentric stages of detector elements. *ATLAS Experiment © 2013 CERN.*

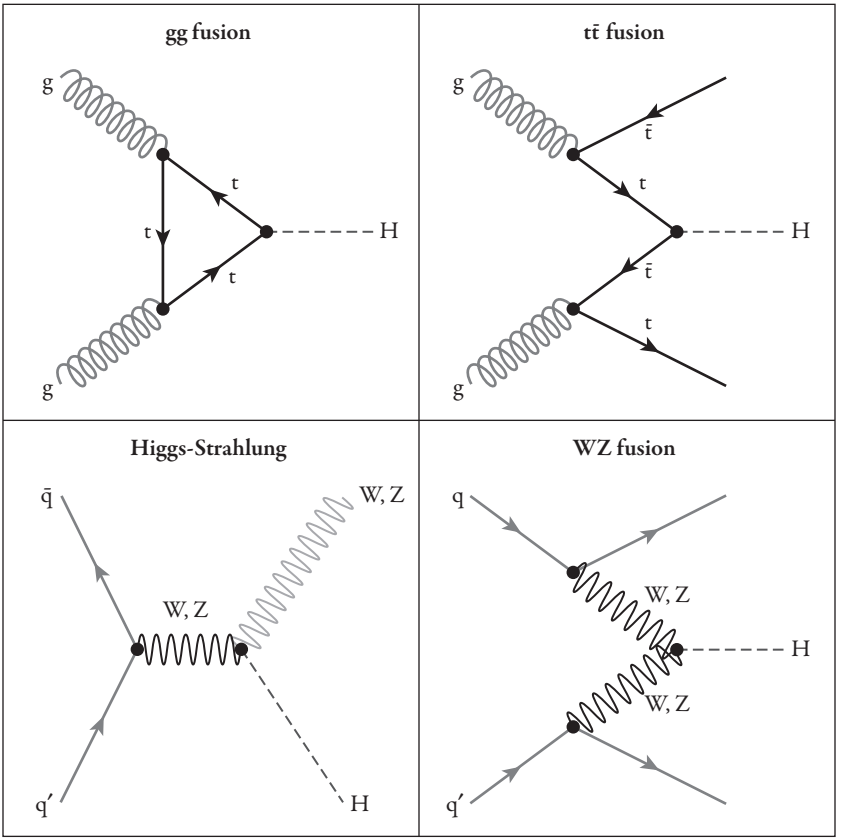

FIGURE 6.5 The mechanisms for production of Higgs (H) particles at CERN. The quarks (q) and gluons (g) inside the protons collide to make Higgs particles. The dominant mechanism is the gluon-gluon fusion displayed in the top-left panel: a top (t) quark loop allows the conversion of two gluons to a Higgs particle. In these diagrams, overbars indicate antiparticles. The primes over the quarks indicate that two different types of incoming quarks may be involved (for example, an up quark from one of the colliding protons and a down quark from the other).

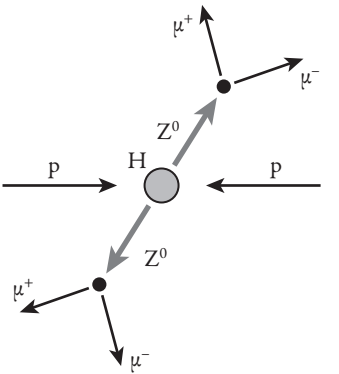

FIGURE 6.6 Collisions of two protons can create a Higgs particle, which then decays into two Z^0 particles. Each of the Z^0 bosons converts to two muons ($\mu^+\mu^-$ as shown) or two electrons. The resulting four particles can be detected in CMS or ATLAS, and the mass of the Higgs can then be reconstructed.

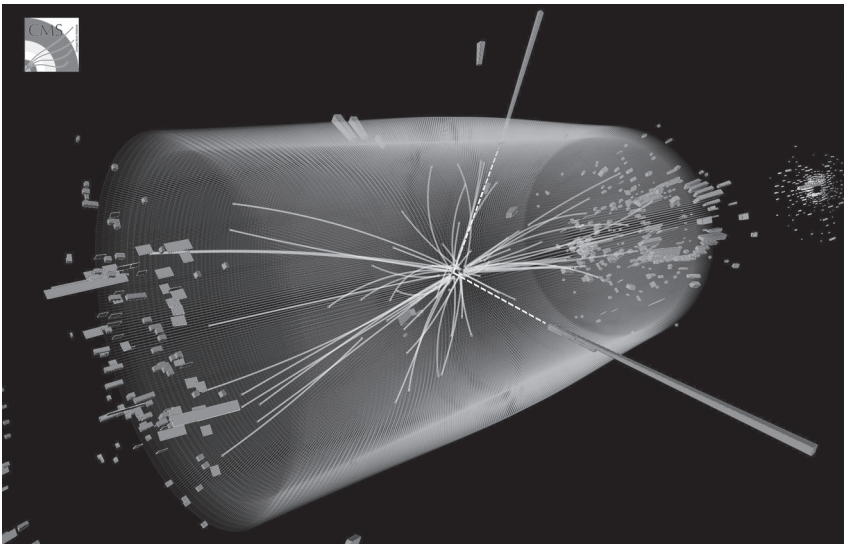

FIGURE 6.7 (A color version of this figure is included in the insert following page 82.) A computer reconstruction of an actual proton-proton collision event using real data recorded with the CMS detector in 2012. The event shows evidence for the decay of a Higgs particle into a pair of photons (in the color version, dashed yellow lines leading to green towers). *CMS and CERN.*

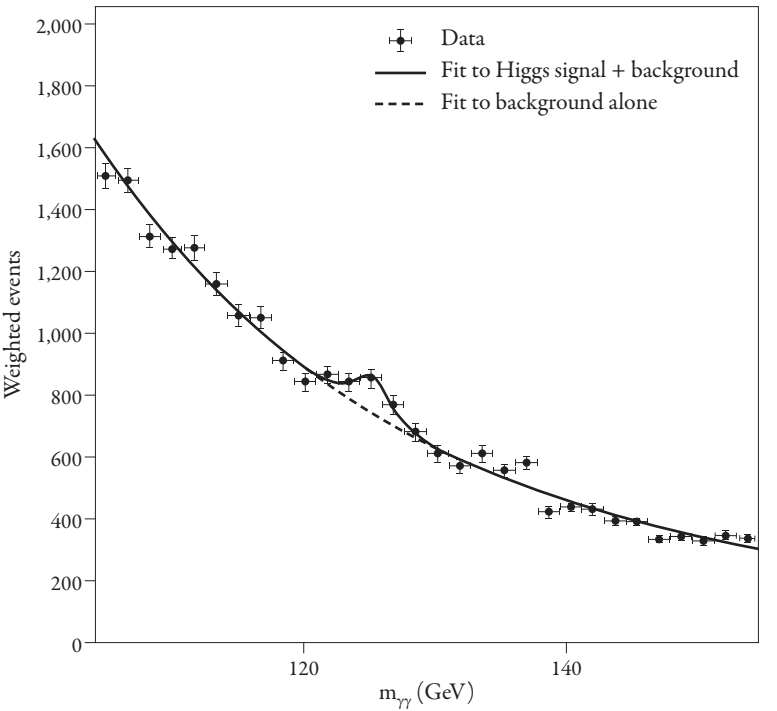

FIGURE 6.8 The discovery of the Higgs particle: the bump in the data taken by the CMS detector at CERN is due to production and decay of a Higgs particle. The black points with error bars indicate the numbers of observed events from high-energy proton collisions into two photon final states, for a variety of values of the two-photon invariant mass $m_{\gamma\gamma}$ (the sum of the energies of the two photons). The solid line shows the fit to the data for Higgs signal plus background noise; the dashed line shows only the background. The bump in the data is caused by a newly discovered Higgs particle with a mass of 125 GeV (125 proton masses). *CMS and CERN.*

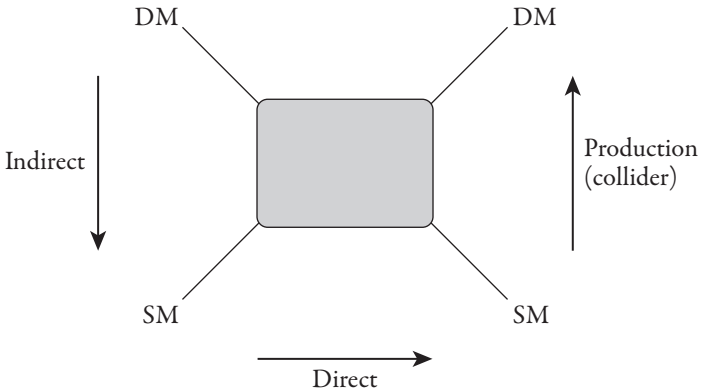

FIGURE 7.1 One diagram illustrates all three prongs of the experimental hunt for dark matter particles. Weakly Interacting Massive Particles (WIMPs), labeled by the letters DM, interact with ordinary matter particles, labeled SM (for the Standard Model of particle physics), via the weak interactions symbolized by the box in the middle of the diagram. The box can represent a variety of mechanisms, including intermediary W bosons, Z bosons, or Higgs bosons. The three arrows indicate the three different detection approaches. The upward-pointing arrow on the right side of the figure illustrates WIMP production in atom smashers such as at CERN in Geneva. In this case, the diagram is read from bottom to top: two protons (labeled SM at the bottom of the diagram) collide with one another to produce outgoing WIMPs (labeled DM at the top of the diagram). Detectors at CERN search for the WIMPs created by this interaction. Alternatively, the arrow that points to the right on the bottom of the diagram illustrates the basic idea of laboratory direct detection experiments. In this case, the diagram is read from left to right. Here a WIMP from the Milky Way Galaxy (DM on the upper left) hits a nucleus in the detector (SM on the lower right), scatters off of it, and deposits a detectable amount of energy. In the end, the WIMP (DM on the upper right) leaves the detector again. The nucleus (SM on the lower right) has gained energy from the interaction, and this energy can be measured. Finally, the downward pointing arrow on the left indicates indirect detection, where the annihilation of WIMPs in space produces energetic photons, neutrinos, and positrons (all from the Standard Model of particle physics) that may be found in detectors here on Earth. In this third detection method, the diagram is read from top to bottom.

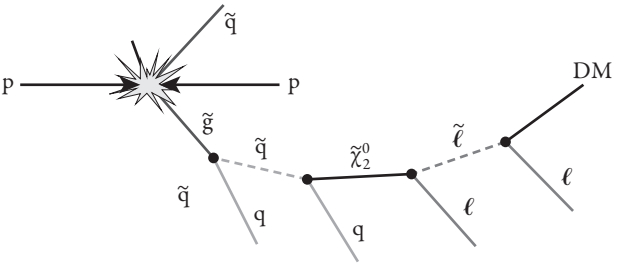

FIGURE 7.2 Signatures of dark matter particles at the Large Hadron Collider will be missing energy plus jets. Because dark matter escapes the detector without interacting, there will be an imbalance in the measured momenta of the final particles in the direction perpendicular to the beam. The quarks and leptons emerging from the decay chain will also produce observable jets of particles, a second signature of dark matter. In the figure the dark matter consists of the lightest supersymmetric particle, symbolized by DM. Tildes over the letters indicate SUSY particles, and the letter ℓ refers to leptons, that is, electrons, muons, or tau particles.

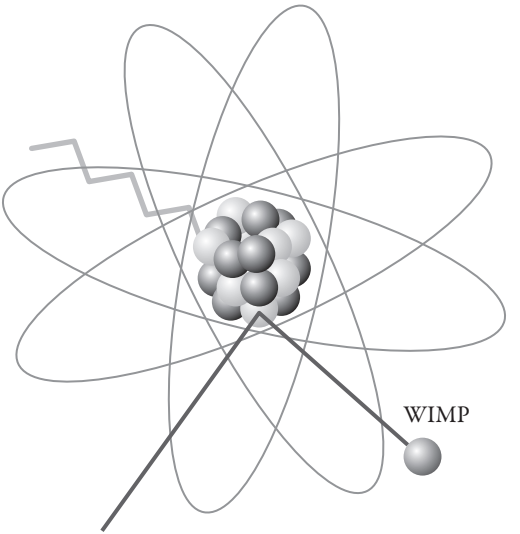

FIGURE 7.3 Direct detection experiments: a Weakly Interacting Massive Particle (WIMP) from the Galaxy scatters off of a nucleus in a detector, leading to a nuclear recoil and small amount of energy deposit that can be measured.

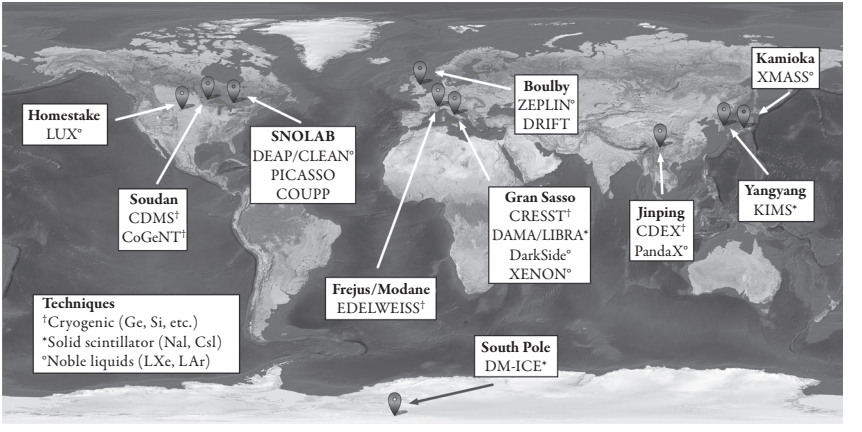

FIGURE 7.6 Underground laboratories (indicated in boldface) are the sites of direct detection dark matter experiments worldwide (experiments listed at their respective locations). These hunt for dark matter by searching for the energy deposited when a WIMP strikes a nucleus in the detector. The key indicates the three types of techniques used in the experiments: cryogenic experiments operating at low temperatures measure the heat deposited by the interaction; solid scintillators absorb the energy and reemit flashes of light; and noble liquids produce scintillation light as well as electrons that later convert to photons. *Michael Woods and Mani Tripathi, University of California, Davis.*

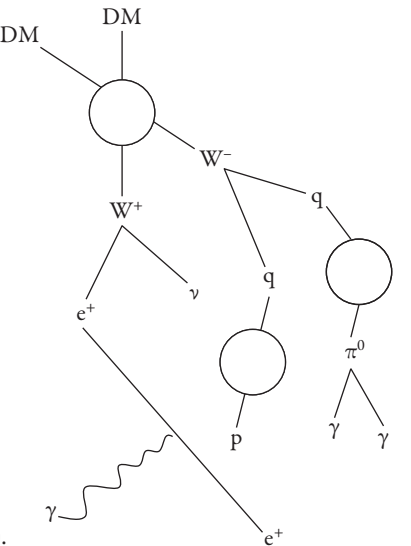

FIGURE 7.7 Indirect detection looks for the final products of annihilation of Weakly Interacting Massive Particles (WIMPs; denoted by DM in the figure). Depending on the model, WIMP annihilations can produce Standard Model fermions, gauge bosons, or Higgs bosons, which then undergo a series of decays, for example, via pions (π^0), to a variety of final particles. Experiments in space and in the ice at the South Pole are searching for three types of final annihilation products: gamma-ray photons (γ), positrons (e^+), and neutrinos (ν).

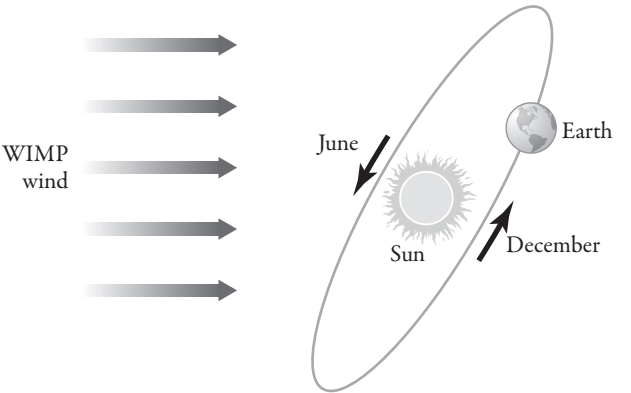

FIGURE 8.1 Earth's orbit around the Sun produces an annual modulation of the Weakly Interacting Massive Particle (WIMP) signal in detectors. The count rate is expected to have a peak in June and a minimum in December.

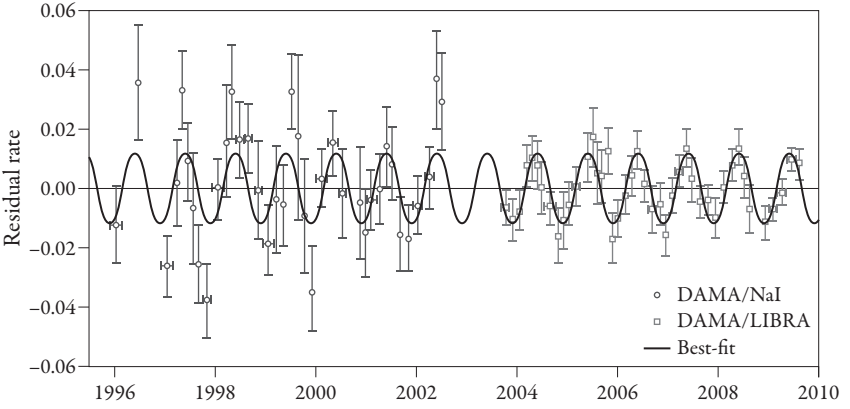

FIGURE 8.2 Direct detection count rates over more than a decade from the DAMA experiment in Italy, showing data points with error bars. The time dependence of the signal is exactly consistent with the annual modulation expected for a Weakly Interacting Massive Particle signal stemming from Earth's motion around the Sun (theoretical predictions are shown by the solid line). The average count rate over the whole time period has been subtracted off, so that only the residuals are plotted. As predicted, the count rate peaks in June and has a minimum in December. *From Bernabei, R., P. Belli, F. Cappella, R. Cerulli, F. Montecchia, F. Nozzoli, A. Incicchitti, and D. Prosperi, et al. 2003. "Dark Matter Search."* Rivista del Nuovo Cimento *26: 1; Bernabei, R., et al. [DAMA and LIBRA Collaborations]. 2010. "New Results from DAMA/LIBRA."* European Physics Journal *C 67: 39*.

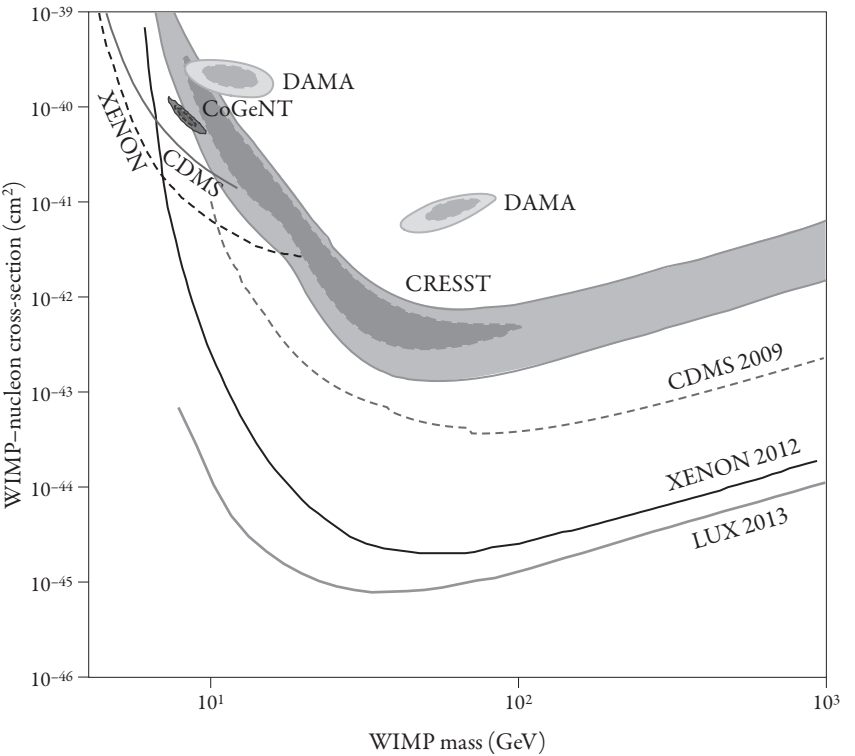

FIGURE 8.3 Comparison of results from a variety of laboratory dark matter experiments for the case of spin-independent Weakly Interacting Massive Particles (WIMPs). The solid zones show regions compatible with the signals observed in the DAMA, CoGeNT, and CRESST experiments. The curves show limits placed by null results (zero signal) of the CDMS and XENON experiments; only regions below these curves are allowed. The null results are clearly in tension with the positive signals, implying either experimental error, incorrect astrophysical halo models, or wrong particle physics assumptions. *Plot made by Joachim Kopp for inclusion in Freese, K., M. Lisanti, and C. Savage. "Colloquium: Annual Modulation of Dark Matter."* Reviews of Modern Physics *85(4): 1561.*

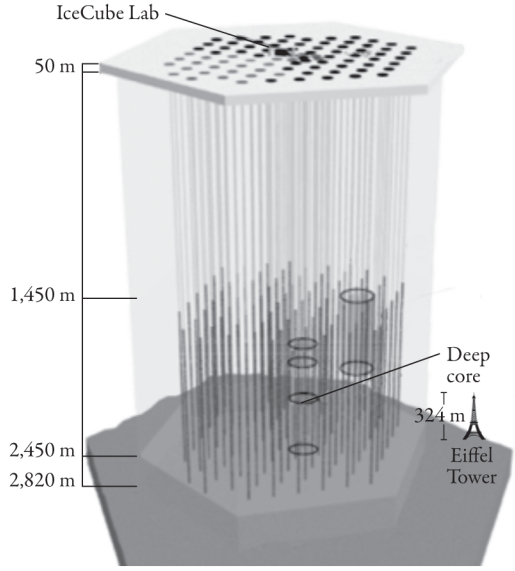

FIGURE 8.7 The IceCube/DeepCore detector at the South Pole consists of kilometer-long strings of phototubes dug deep into the ice. The Eiffel Tower is shown for comparison. On the right is a postcard of a penguin I received from Antarctica. *(Right) pinguino k.*

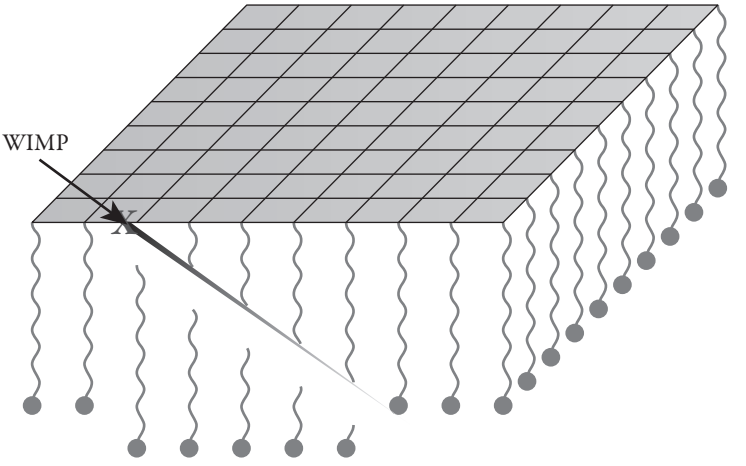

FIGURE 8.8 A novel idea for dark matter detectors using DNA. A Weakly Interacting Massive Particle (WIMP) from the Galaxy hits a thin foil of gold and knocks a gold nucleus into hanging strands of DNA. The gold severs any DNA strand it hits. Biologists can identify the location where the DNA broke off and reconstruct the track of the recoiling gold nucleus (with nanometer accuracy). Because the WIMP scatters the gold in the forward direction, this technique identifies the path of the incoming WIMP. *From A. Drukier, K. Freese, D. Spergel, C. Cantor, G. Church, and T. Sano. "New Dark Matter Detectors Using DNA for Nanometer Tracking." arXiv:1206.6809 [astro-ph.IM].*

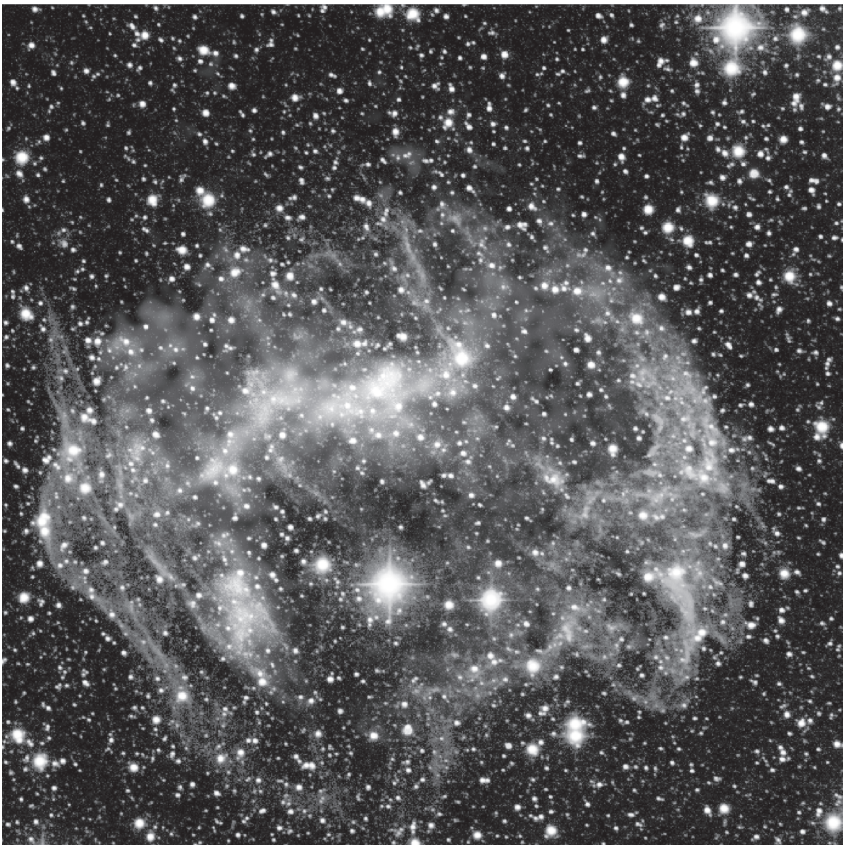

FIGURE 9.1 (A color version of this figure is included in the insert following page 82.) A supernova remnant. *(X-ray) NASA/CXC/SSC/J. Keohane et al.; (infrared) Caltech/SSC/J. Rho and T. Jarrett.*

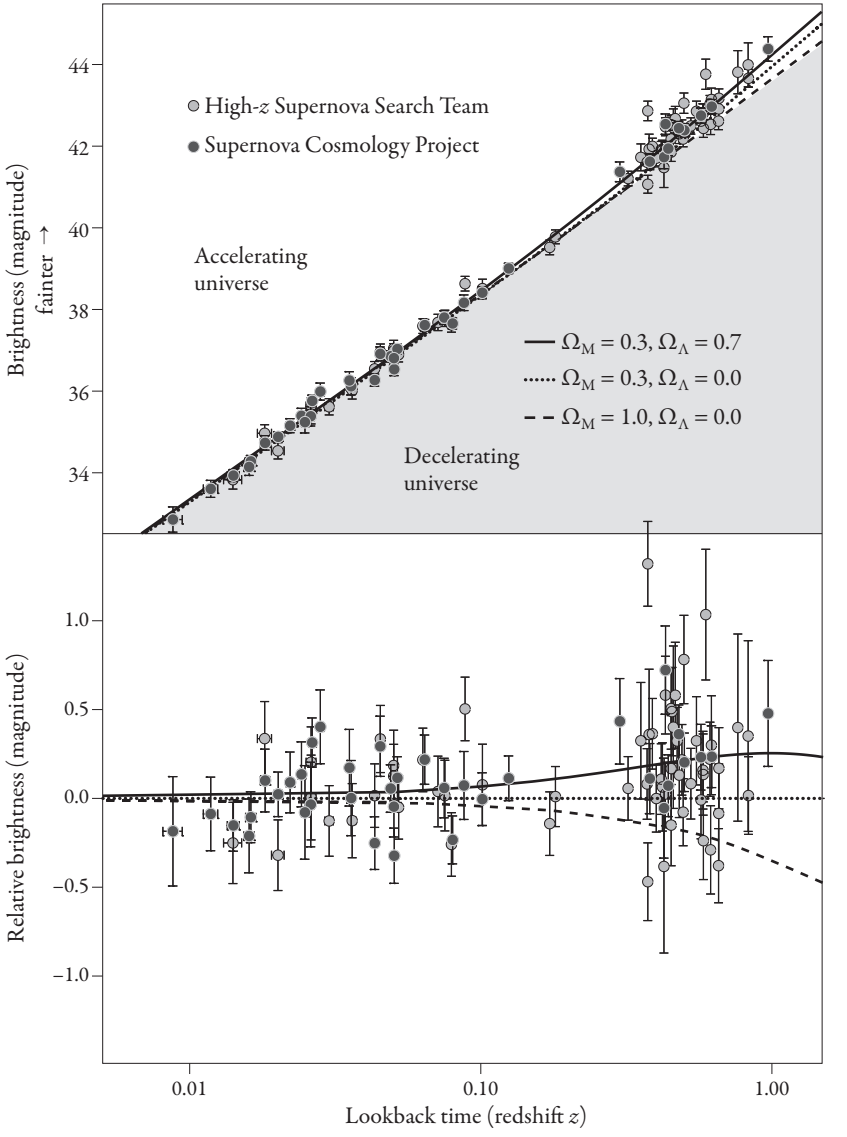

FIGURE 9.2 The supernova data that proved that the Universe is accelerating. The upper panel shows the brightness of Type IA supernovae at different redshifts, or lookback times. Effectively this is a plot of the distance to the supernovae versus the time of the explosions. The 1998 data (dots with error bars) were taken by the High-z Supernova Search Team and the Supernova Cosmology Project. The data tilt upward, indicating that the Universe is accelerating. Both plots show comparison of the 1998 Type IA supernova data to a variety of hypothetical universes with varying contributions from matter and dark energy. The bottom panel shows the difference between data and models from the $\Omega_M = 0.3$ and $\Omega_\Lambda = 0$ prediction. The best fit to the data requires

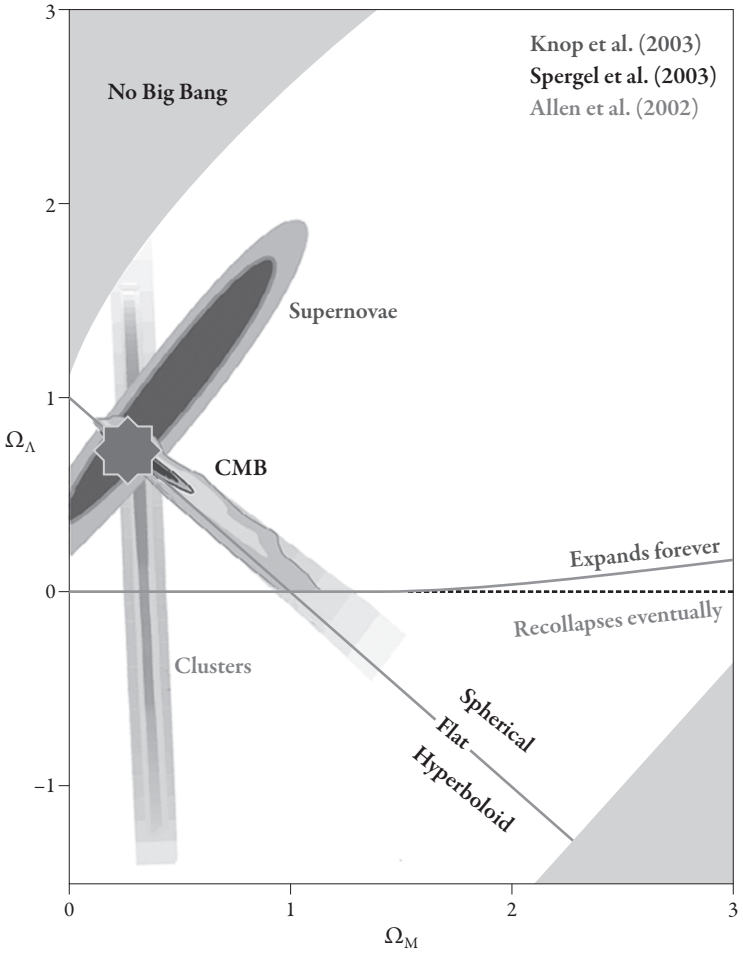

FIGURE 9.3 (A color version of this figure is included in the insert following page 82.) A variety of astrophysical data sets converge on a Universe with 31% matter and 69% dark energy. The horizontal axis is the fraction of the Universe consisting of matter (both atomic and dark matter), and the vertical axis is the fraction consisting of dark energy. In the color version of the figure, the green regions are consistent with supernova data; the red regions with cluster data; and the brown regions with cosmic microwave background (CMB) data. The best fit that matches all the data (indicated by a star) is 31% matter and 69% dark energy. Although this figure doesn't make the distinction, the matter content is further divided into 5% atomic matter and 26% dark matter.

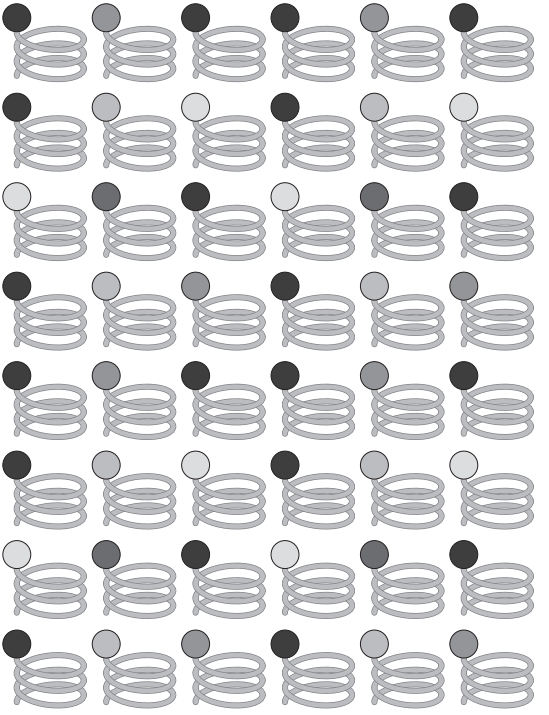

FIGURE 9.5 Quantum field theory description of the vacuum.